Int. Journal of Refractory Metals and Hard Materials 29 (2011) 608–613

Contents lists available at ScienceDirect

Int. Journal of Refractory Metals and Hard Materials

journal homepage: www.elsevier.com/locate/IJRMHM

Tensile properties and strengthening mechanisms of Mo–Si alloy

Zhang Guo-jun [a,b,*], Lin Xiao-hui [a], Wang Rui-hong [a], Liu Gang [b], Sun Jun [b]

[a] School of Materials Science & Engineering, Xi'an University of Technology, Xi'an, 710048, PR China
[b] State Key Laboratory for Mechanical Behavior of Materials, Xi'an Jiaotong University, Xi'an, 710049, PR China

ARTICLE INFO

Article history:
Received 19 January 2011
Accepted 15 April 2011

Keywords:
Mo–Si alloy
Tensile property
Strengthening mechanisms
Strengthening model

ABSTRACT

Pure Mo and Mo–Si alloys with different silicon content were fabricated by powder-metallurgical and thermo-mechanical processing. Tensile properties of the pure Mo and Mo–Si alloys were measured at room temperature and the fracture surface was analyzed after test. The results indicate that Si can effectively reduced the grain size and improve the yield strength of Mo–Si alloys. With the decrease in grain size, the dominant fracture morphology is changed from intergranular to transgranular. The strengthening mechanisms were discussed and the yield strength was analyzed described with respect to grain size, solid solution hardening and Mo_3Si particle strengthening. Calculations show that the yield strength of Mo–Si alloys is governed by grain size.

© 2011 Elsevier Ltd. All rights reserved.

1. Introduction

Molybdenum boronsilicides are potential materials for ultra-high temperature structural components because of their outstanding combination properties, such as high melting point, high-temperature strength and excellent high temperature oxidation resistance [1,2]. Usually, Mo–Si–B alloys compose of three phases: solid solution phase Mo_{ss} and brittle intermetallic phases Mo_5SiB_2 (T_2 phase) and Mo_3Si. The two intermetallic phases are very strong at high temperatures and provide the necessary oxidation resistance above 1000 °C. While the Mo_{ss} is not oxidation-resistant, it has excellent ductility and toughness that are very important for improve the fracture toughness of molybdenum borosilicide alloys. Recent studies have been frequently focused on the Mo_{ss}-rich multiphase Mo–Si–B alloys [3,4].

According to previous studies [5], the solubility of Si in Mo is 3 at.% at 1600 °C in binary Mo–Si alloy, while the solubility of B in Mo is thought to be negligible at room temperature. Its effect on the mechanical properties of the solid solution molybdenum alloy is thought to not be critical [6]. Sturm et al. [7] studied Mo-rich Mo–Si alloys produced by hot press sinter processing and found that the calculated solid solution strengthening was 97 MPa and that is much lower than the measured yield strength difference between Mo-1.0Si and pure Mo of ≈500 MPa. It is indicated that the strength increase in Mo–Si alloy is related not only to the solid solution strengthening but also to the grain size and Mo_3Si particles, which are separated from supersaturate Mo lattice because of lower solubility of Si in Mo, some early studies indicates that the solubility of Si in Mo at ~1100 °C was reported as only 0.21 wt.% and decreased with temperature fall down [8]. So, the solid solution strengthening mechanism is not enough to explain the pronounced strengthening effect of Si in Mo. However, previous work has not reported the systematical investigations on the coupling effect of various strengthening mechanisms on the strength of Mo–Si alloys. This work is aimed at investigating the mechanical properties of Mo_{ss}-rich Mo–Si alloys. Especially, we try to establish a quantitative relationship between microstructure parameters and mechanical properties.

2. Experimental procedures

In the present study, pure Mo, Mo-0.1wt.%Si, Mo-0.3wt.%Si were prepared by powder-metallurgical and thermo-mechanical processing. Elemental powders of Mo and Si are 99.96 wt.% and 99.5 wt.% purity, respectively. For each alloy, 2 kg of powder was mixed. A milling process was carried out for 48 hour in a stainless steel container with Mo milling balls in a planetary ball mill with a rotational speed of 40 rpm. Homogeneously mixed powders were statically cold pressed into slab compacts, and sintered at 1900 °C for 6 hour in flowing dry hydrogen. The resulting sinter billets were then thermo-mechanically processed at 1330–1270 °C into sheets with the thickness over 2.5 mm (ε 80%) and cooling in dry hydrogen atmosphere. Finally, the pure Mo sheets and Mo–Si alloy sheets were annealed at 900 °C for 1 hour and 1050 °C for 1 hour and furnace cooling in vacuum, respectively, to release residual stress and stabilize the microstructure. In order to investigate the grain size effect on mechanical properties, the Mo–Si sheets were also annealed at 1350 °C for 3 hour.

Optical microscopy (OM) observations were performed by using an OLYMPUS GX71 metalloscope. Grain sizes were determined using average linear intercept method on polished and etched specimens. For each alloy, more than 10 pictures were countered in order to

* Corresponding author at: School of Materials Science & Engineering, Xi'an University of Technology, Xi'an, 710048, PR China. Tel.: +86 29 8231 2592; fax: +86 29 82312994.
E-mail address: zhangguojun@mail.xjtu.edu.cn (Z. Guo-jun).

0263-4368/$ – see front matter © 2011 Elsevier Ltd. All rights reserved.
doi:10.1016/j.ijrmhm.2011.04.006

obtain an accurate value. The dog-bone shaped tensile specimens having a gage size of 30 mm in length and 2.5 mm in thickness and 8 mm in width were fabricated from the annealed sheets by electrical discharge machining. Prior to testing, the ends of the samples were ground and polished flat and parallel to each other. Tensile testing was carried out at room temperature in air at a constant strain rate of 1.1×10^{-3}/s using a servo-hydraulic Instron-1195 testing machine. The fracture morphology of tensile specimens was examined using a JSM-6700 F field emission scanning electron microscope (SEM). The microstructure of the alloy was observed using a JEM-3010 transmission electron microscopy (TEM). The thin foils were obtained using twin-jet electropolishing in a solution of 5% butyl alcohol, 5% perchloric acid and 90% ethanol at 30 V and −30 °C.

3. Results

3.1. Optical microstructure observation

The micrographs of pure molybdenum and Mo–Si alloys before and after annealed at different temperature in vacuum are shown in Figs. 1 and 2. Compare to Fig. 1a, the microstructure of pure Mo is gradually widened after annealed at 900 °C, but still exhibited the rolling trace (seen in Fig. 2a). After being annealed at 1050 °C, the Mo-0.1Si alloy has finer grains than pure Mo, with some equiaxial grains present in fibrous structure (Fig. 2b). Although the Mo-0.3Si sheet is annealed at the same temperature, the grains remain fully fibrous and elongated pattern (Fig. 2d). For the Mo–Si alloys annealed at 1350 °C for 3 h (Fig. 2c and e), the grains change to equiaxial.

The measurements of grain sizes for pure Mo and Mo–Si alloys are listed in Table 1. It is clearly revealed that the addition of Si has remarkable effect on the grain size, i.e., the presence of Si can suppress the grain growth during the rolling and annealing treatment.

3.2. Mechanical property

Typical room-temperature stress–strain curves of pure Mo and Mo–Si alloys annealed at different temperature were shown in Fig. 3. One can find that, although the Si mass fraction is tiny, the yield strength and ultimate tensile strength (UTS) of Mo–Si alloys annealed at similar temperatures were obviously higher than pure Mo. Compared with pure Mo, the Mo–Si alloys show a visible work-hardening trend. The ductility of Mo–Si alloy is lower than pure Mo when the content of Si is 0.1 wt.%, however, when the Si content is increased to 0.3 wt.%, the samples have a large elongation and show necking behavior before failure.

At higher annealing temperature and longer annealing time, i.e., annealed at 1350 °C for 3 hour, the yield strength and ultimate tensile strength of the Mo–Si alloy are decreased and the ductility is also greatly reduced. Coarse grains will be responsible for the weakling effect in mechanical properties. The results of room temperature tensile test for pure Mo and Mo–Si alloys sheet are list in Table 2.

From Table 2, it can be noted that the solid solution softening in Mo–Si alloy that reported by D. Sturm et al.[7] did not appear in our present work. In their study, the hardness and yield stress of hot pressure sinter billet of Mo–Si alloy decreased at 0.1 wt.% Si concentration, they called that solid solution softening or alloy softening. The solid solution softening in bcc metals has previously been reported by Arsenault [9]. According to their work, the Mo–Re and Mo–Pt exhibited the solid solution softening. However, there had been only one report so far of solid solution softening in the Mo–Si system before the work of D. Sturm et al. In that report the Vickers hardness of Mo-0.03 wt.% Si was found to be lower than the pure Mo. In order to explain this phenomenon, Trinkle and Woodward [10] developed a quantitative model of alloy softening based on quantum-mechanical calculations and they found that the outstanding characteristic of those elements which Mo have higher d electron numbers (e.g. Re have 5 electrons in 5 d, Pt have 9 electrons in 5 d). The element of Si has no d electron [11] and therefore should not cause softening behaviors.

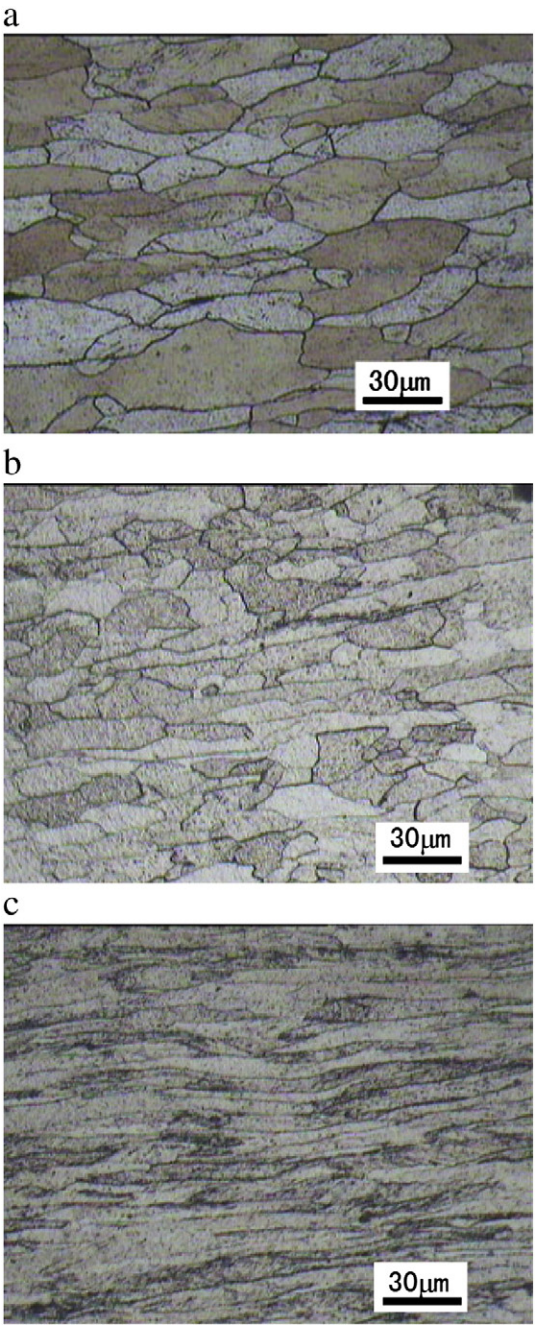

Fig. 1. Optical images of rolling Mo–Si alloys before vacuum annealing treatments (a) Pure Mo; (b)Mo-0.1Si; (c)Mo-0.3Si.

3.3. Fracture surface

Tensile fracture surface of the pure Mo and Mo–Si alloy annealed at different temperature were shown in Fig. 4. It is apparently that the pure Mo fractured completely by cleavage and it has a very slight deformation in grain boundaries. After annealed at 1050 °C for 1 hour, the Mo-0.1Si alloy sample showed a fracture surface of transgranular and intergranular mixed mode, where the dominant morphology is transgranular. After annealed at 1350 °C for 3 hour, the Mo-0.1Si alloy with coarse grains has also the mixed fracture mode, while the dominant morphology becomes intergranular. The

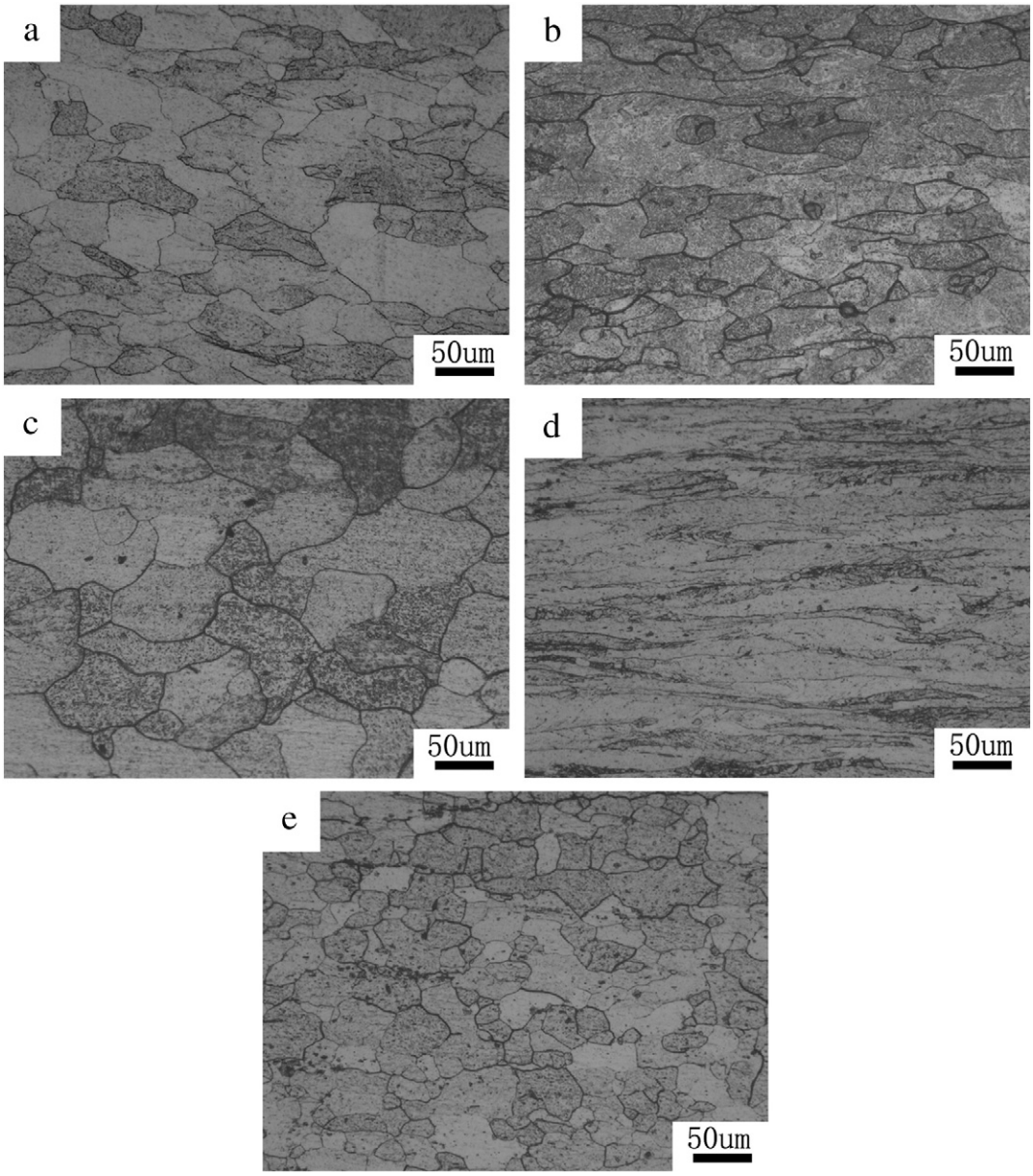

Fig. 2. Optical images of Mo–Si alloys after vacuum annealing treatments for 1 hour (a) Pure Mo at 900 °C; (b) Mo-0.1Si at 1050 °C; (c) Mo-0.1Si at 1350 °C; (d) Mo-0.3Si at 1050 °C; (e) Mo-0.3Si at 1350 °C.

Mo-0.3Si alloy which annealed at 1050 °C for 1 hour exhibit fracture surface different from other samples, as seen in Fig. 4(d), the sample exhibit a woody fracture, there are some small dimples distributed in tear ridges and some cracks between grains that were vertical to applied stress direction. This structure displays an excellent ductility during deformation. The fracture mode of Mo-0.3Si alloy, annealed at 1350 °C for 3 hour, was dominated by intergranular fracture, which is similar to Mo-0.1Si alloy treated under the same condition.

Table 1
Grain sizes of pure Mo, Mo-0.1Si and Mo-0.3Si alloys before and after vacuum annealing treatment.

Material	Grain size(μm)			
	Before annealed	900 °C, 1 hour	1050 °C, 1 hour	1350 °C, 3 hour
Pure Mo	13.2	21.2	–	–
Mo-0.1Si	11.4	–	19.5	44.3
Mo-0.3Si	7.0	–	12.2	22.4

4. Discussion

The microstructure analyses show that the Si content has notable effect on the grain size. Besides, from the binary phase diagram of Mo–Si, the solubility of Si in Mo is very small. In addition, Mo3Si particles will be produced with increasing Si content and these particles can hinder dislocation movement as obstacles (Fig. 5). Thus, the strengthening mechanisms in the Mo–Si alloy sheets should include three components: grain boundary strengthening, solid solution strengthening, and particles strengthening. The yield strength of the Mo–Si alloy sheet can be quantitatively described as the superimposition of matrix intrinsic strength, fine-grain strengthening term, solid solution strengthening term and particle strengthening term, i.e.[12],

$$\sigma_y = \sigma_0 + \sigma_f + \sigma_s + \sigma_{OR} \quad (1)$$

Where σ_y is the total yield strength of Mo–Si alloy, σ_0 is the matrix intrinsic strength of the material (the strength of an large grain size of

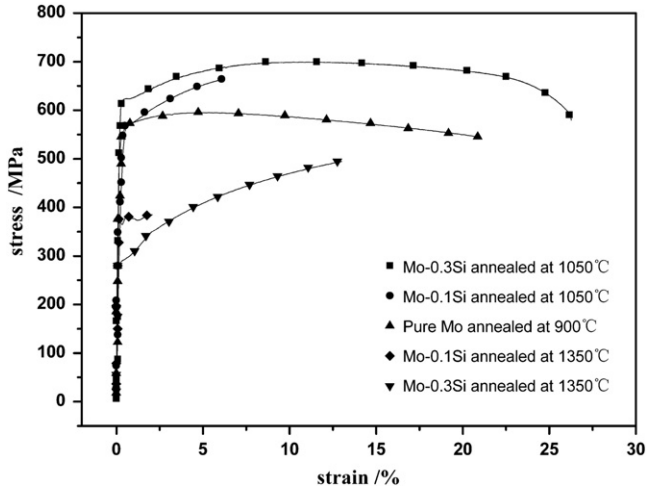

Fig. 3. Stress–strain curves for room temperature tensile tests of the pure Mo and Mo–Si alloys.

material), σ_f is the strength related directly to grain size and can be formulated by Hall-Petch relation, σ_s is the strength contributed by Si solutes, and σ_{OR} is the strength come from the Mo_3Si particles and can be explained by the Orowan model.

4.1. Fine-grain strengthening

Dependence of yield stress on the grain size can be referred to the well-known Hall–Petch relationship:

$$\sigma = \sigma_0 + K / d^{1/2} \tag{2}$$

Where σ is the summation of the matrix strength and fine-grain strength, K is the Hall–Petch constant, and d is the grain size. K can be evaluated using the experimental results of pure Mo. Taking $\sigma = 549.3$ MPa (Table 2) and $\sigma_0 = 417$ MPa [13], K is determined as 608.4 MPa·μm$^{1/2}$ according to the measurement of d (Table 1). We can now put the value of K into Eq. (3) to see the fine-grain strengthening contribution in Mo-0.1Si and Mo-0.3Si alloys by using the measured grain size.

$$\sigma_f = K / d^{1/2} \tag{3}$$

4.2. Solid solution strengthening

About solid solution strengthening, there is an equation given by Vöhringer hold well for solid solution strengthening contribution in copper:

$$\sigma_s = M \times \left(\frac{G}{550}\right) \varepsilon_L^{4/3} c^{2/3} \tag{4}$$

Table 2
The results of room temperature tensile test for pure Mo and Mo–Si alloys.

Material	Annealing temperature and time	0.2% yield stress (MPa)	UTS (MPa)	Elongation (%)
Pure Mo	900 °C, 1 h	549.3	595.1	20.9
Mo-0.1Si	1050 °C, 1 h	562.7	664.5	6.3
Mo-0.1Si	1350 °C, 3 h	364.9	385.0	2.1
Mo-0.3Si	1050 °C, 1 h	621.6	699.4	26.3
Mo-0.3Si	1350 °C, 3 h	288.2	494.3	13.0

Where M is the Taylor factor, G is the shear modulus, c is the solute mole fraction, and ε_L is:

$$\varepsilon_L = \sqrt{(15\varepsilon_b)^2 + \left(\frac{\varepsilon_G}{1 + |\varepsilon_G|/2}\right)^2} \tag{5}$$

Where ε_b and ε_G represent the atomic size and modulus misfit and given by: $\varepsilon_b = (R' - R)/R$, $\varepsilon_G = (G' - G)/G$, respectively [14]. Where R' and R represent the atomic radius of Si and Mo, G' and G represent the shear modulus of Si and Mo. Following the study of Sturm et al., Eq. (4) was employed to assess the increase in yield stress due to solid solution strengthening in the Mo–Si alloys. In their work, they assumed the M as 3.1, which is constant data for fcc metal, while in bcc metal M was generally taken as 2.0 [14]. In addition, the solubility of Si in Mo at room temperature is not well known but is anticipated to be low and the solubility at ~1100 °C was reported as 0.21 wt.% [8]. But the contribution from solid solution strengthening is not so remarkable, we can see that the increase in Si solubility from 0.1 wt.% to 0.2 wt.% cause a corresponding strength increase from 34.5 MPa to 54.8 MPa by calculated from Eqs. (4) and (5), with a difference of only 20 MPa. So the solubility of Si is not significant to the strengthening effect, 0.15 wt.% will be simply chosen as the standard solubility of Si in Mo at room temperature in present work. With the $\varepsilon_b = -0.16$ [15], $\varepsilon_G = -1.7$, $G = 117$ GPa [7] and $M = 2.0$, the increase in yield strength due to solid solution strengthening can be calculated as shown in Table 3.

4.3. Particle strengthening

With increasing of Si content, some Mo_3Si particles are produced as shown in Fig. 4. Based on the assumption above, there will be 0.15 wt.% Si was separated as Mo_3Si particle in Mo-0.3Si alloy. According to the well-known Orowan–Ashby equation, the increase in yield strength due to Mo_3Si particle strengthening was represented as follows [16–18]:

$$\sigma_{OR} = \frac{MGb}{1.18 \times 2\pi \times \phi\left(\sqrt{\pi/6f} - 1\right)} \ln\left(\frac{\phi}{2b}\right) \tag{6}$$

Where M is the Taylor factor taken as 2.0 in bcc structure [13], G is the shear modulus as 117 GPa, b is the Burgers vector (110) 111 as 0.237 nm, f is the volume fraction of Mo_3Si particle which can be calculated as 1.913%, and ϕ, the particle size was statistic from our previous work as 0.5 μm. The result was also list in Table 3.

From the above quantitative assessments, it can be clearly seen that the contribution of the grain refining on the total yield strength is about 132.3–174.3 MPa for the range of grain size studied here and it is evidently higher than the contributions of both the solid solution and particles. The lower solubility of Si in Mo and the Mo_3Si particle with sub-micron in size are the reasons for little contribute of solid solution strengthening and particle strengthening. The reduced grain size not only contributes to strength but also improve the toughness of Mo–Si alloy. It is thus reasonable to assume that the toughness of Mo–Si–B alloy will be promoted because the grain size was refined by the presence of Si. In addition, because the amount of Mo_3Si particles is tiny and the size is in sub-micron, the strength of Mo-0.3Si alloy come from particles strengthening term is much lower than fine grain strengthening term, but it can be speculated that the lager number of fine Mo_3Si particles in Mo–Si–B alloy will improve the strength dramatically.

Summing the three parts together, the calculated yield strength of the studied Mo–Si alloys are shown in the Fig. 6 to compare with the experimental data. The calculations are in good agreement with the experimental results. There are approximately +4.7% and +7.0%

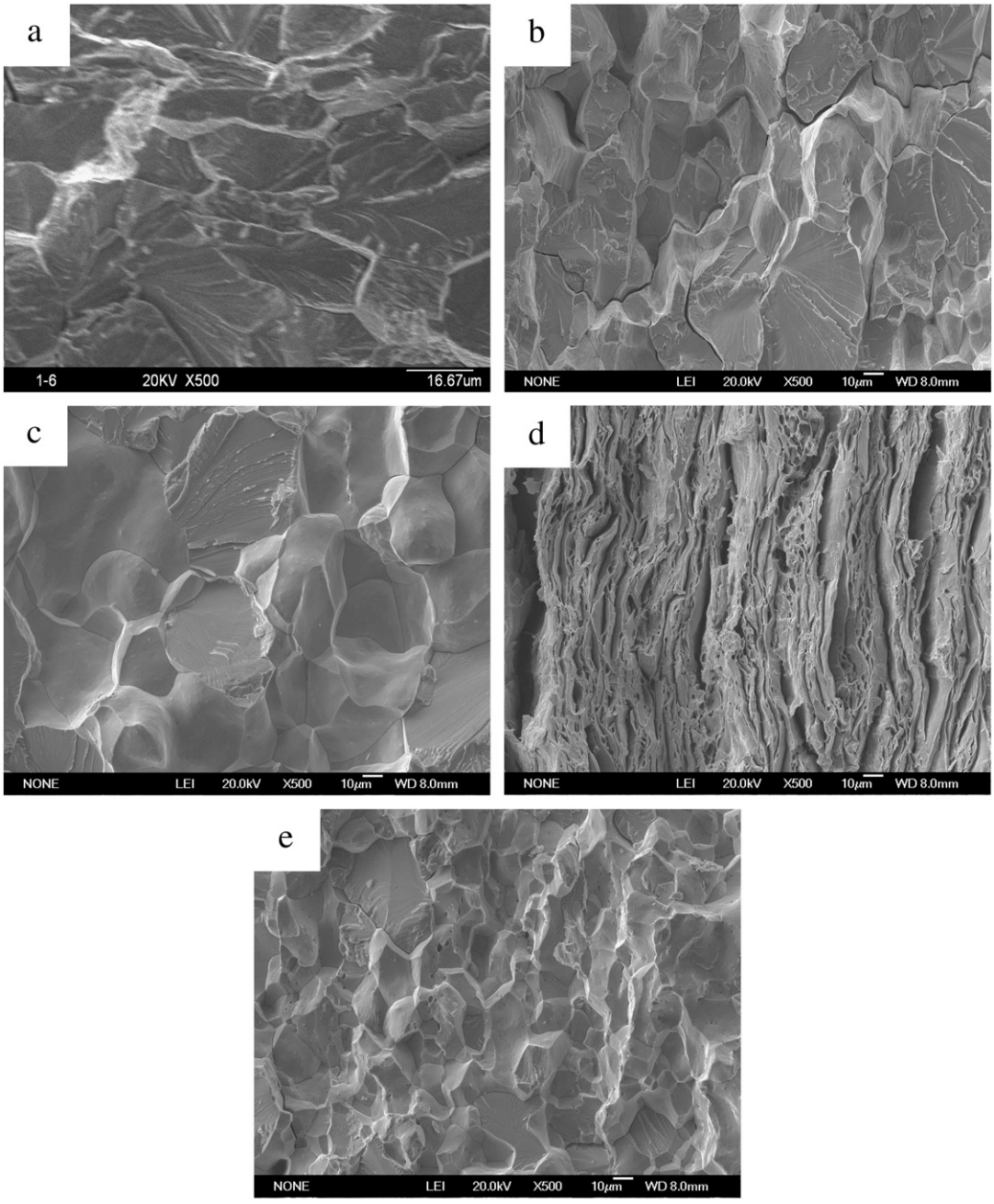

Fig. 4. SEM image of fracture surfaces for room temperature tensile tests of Mo–Si alloys sheet which after vacuum annealing treatments for 1 h. (a) Pure Mo at 900 °C; (b) Mo-0.1Si at 1050 °C; (c) Mo-0.1Si at 1350 °C; (d) Mo-0.3Si at 1050 °C;(e) Mo-0.3Si at 1350 °C.

deviation between calculation and experimental data in Mo-0.1Si and Mo-0.3Si alloy, respectively. The calculations obtained in present work are slightly higher than experimental data, which may be due to following reasons: (a) the theoretical calculation is based on ideal state of materials, while the practical materials contain some sintering and rolling defects more or less, such as microcrack, which will reduce the mechanical properties to some extent; (b) because each of strengthening mechanism is not independent during deformation, the superposition law of fine grain, solid solution and particle strengthening can not described the total yield strength very well only by the simple linear addition. For instance, according to the study on additivity of solid solution and dispersion strengthening by Lagerpusch et al. [19], the total critical resolved shear stress (CRSS)τ_t, the CRSS of solid solution strengthening τ_s and the CRSS of dispersion strengthening τ_p followed the relationship as $\tau_t^k = \tau_s^k + \tau_p^k$ with $k \approx 1.8$ in copper-rich copper-gold solid solution dispersion strengthened by incoherent SiO_2-particles. Eq. (1) needs some further modification by accounting for the interaction between the three strengthening mechanisms, which will be discussed elsewhere.

5. Conclusions

The present of Si can significantly refine the grain sizes and improve the yield strength of Mo–Si alloys. With the coarsening of grain size, both the room temperature yield strength and ductility of Mo–Si alloy decreased precipitously. The solid solution softening in Mo–Si alloy was not observed in our present work. The fracture surface of Mo–Si alloy is found to transit from dominantly transgranular to dominantly intergranular with increasing grain size. The woody structure of Mo–Si alloy displays an excellent ductility. Quantitative analyses indicate that fine

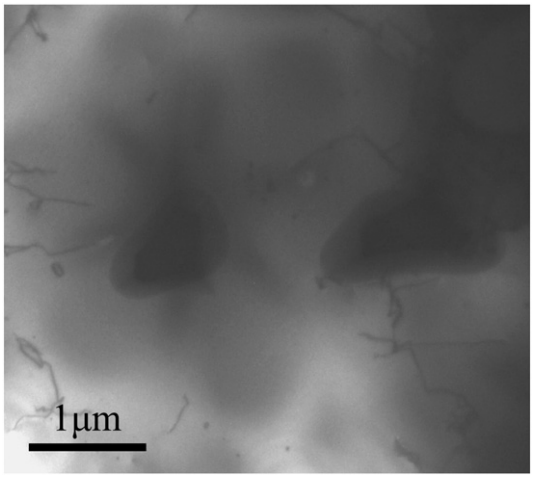

Fig. 5. TEM bright-field image of dislocations were trapped by Mo_3Si particles in Mo-0.3Si.

Table 3
The calculated yield strength of Mo–Si alloys contributed by different mechanisms.

Material	σ_0 (MPa)	σ_f (MPa)	σ_s (MPa)	σ_{OR} (MPa)	σ_y (MPa)	Experimental data
Pure Mo	417	132.3	–	–	549.3	549.3
Mo-0.1Si	417	137.7	34.5	–	589.2	562.7
Mo-0.3Si	417	174.3	45.3	28.3	664.9	621.6

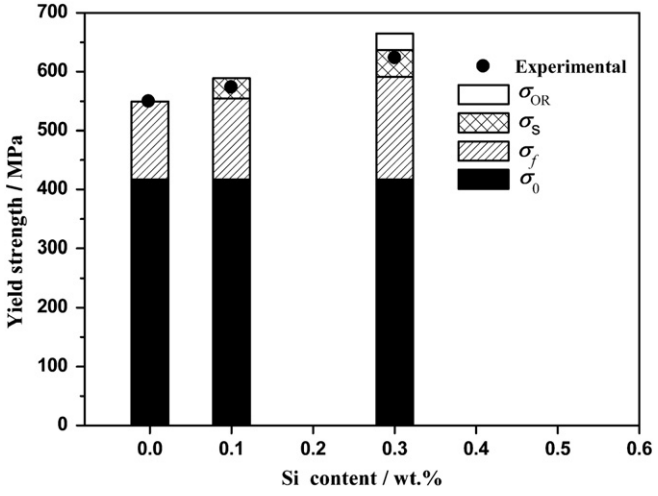

Fig. 6. The all kinds of strengthening contribute to total yield strength of Mo–Si alloys.

grain, solid solution and particle strengthening are main strengthening mechanisms in Mo–Si alloys and the dominant one is the fine grain strengthening. The superposition law of fine grain strengthening, solid solution strengthening and particle strengthening in Mo–Si alloy yields calculations in good agreement with the experimental data.

Acknowledgments

This study was supported by the National Natural Science Foundation (Grant No. 50801051), the National High-technology Research and Development Program of China (Grant No. 2008AA031001) and the Program for New Century Excellent Talents in University (Grant No. NCET-10-0876). The authors also wish to thanks for the work from the State Key Laboratory for Mechanical Behavior of Materials and Jinduicheng Molybdenum Co. Ltd. of China.

References

[1] Akinc M, Meyer MJ, Kramer AJ, Thom JJ, Huebsch, Cook B. Boron-doped molybdenum silicides for structural applications [J]. Mater Sci Eng A 1999;261:16–8.
[2] Choe H, Schneibel JH, Ritchie RO. On the fracture and fatigue properties of Mo-Mo3Si-Mo5SiB2 refractory intermetallic alloys at ambient to elevated temperatures (25°C to 1300°C) [J]. Metall Mater Trans A 2003;34:225–31.
[3] Nieh TG, Wang JG, Liu CT. Deformation of a multiphase Mo–9.4Si–13.8B alloy at elevated temperatures[J]. Intermetallics 2001;9:73–9.
[4] Schneibel JH, Kramer MJ, Easton DS. A Mo-Si-B intermetallic alloy with a continuous α–Mo matrix [J]. Scripta Mater 2002;46:217–21.
[5] Jain P, Alur AP, Kumar KS. High temperature compressive flow behavior of a Mo–Si–B solid solution alloy[J]. Scripta Mater 2006;54:13–7.
[6] Jain P, Kumar KS. Dissolved Si in Mo and its effects on the properties of Mo–Si–B alloys[J]. Scripta Mater 2010;62:1–4.
[7] Sturm D, Heilmaier M. The influence of silicon on the strength and fracture toughness of molybdenum [J]. Mater Sci Eng A 2007;463:107–14.
[8] Perepezko JH, Sakidja R, Kim S, Dong Z. In: Jackson Hole WY, Hemker KJ, editors. Proceedings of the international symposium on structural intermetallics. Warrendale (PA): TMS; 2001. p. 505.
[9] Esterling DM, Arsenault RJ. Arsenault. Peierls-Nabarro Plastic Deformation in the Presence of solute Clusters [J]. Metall Trans A 1982;08(13A):1429–34.
[10] Trinkle DR, Woodward C. The chemistry of deformation: how solutes soften pure metals [J]. Science 2005;310:1665–7.
[11] Callister Jr William D. Materials Science and Engineering an Introduction. 7th Ed. New York: John Wiley & Sons, Inc. press; 2007. p. 22.
[12] Zhang GJ, Sun YJ, Zuo C, Wei JF, Sun J. Microstructure and mechanical properties of multi-components rare earth oxide-doped molybdenum alloys[J]. Mater Sci Eng A 2008;483–4:350–2.
[13] Zhang GJ, Sun YJ, Niu RM, Sun J, Wei JF, Zhao BH. Microstructure and strengthen mechanism of oxide lanthanum dispersion strengthened mo alloy. Adv Eng Mat 2004;6:943–8.
[14] Zhang JS. Strength of Materials. Harbin: Harbin Institute of Technology press; 2004.
[15] Zhang HA. and its composites. Changsha: National Defense Industry Press; 2007.
[16] Kelly A, Nicholson RB. Strengthening methods in crystals [M]. New York: Elsevier; 1971. p. 16–52.
[17] Zhu AW, Starke Jr EA. Strengthening effect of unshearable particles of finite size: a computer experimental study [J]. Acta Mater 1999;47:3263–9.
[18] Zhu AW, Chen J, Starke Jr EA. Precipitation strengthening of stress-aged Al-xCu alloys [J]. Acta Mater 2000;48:2239–46.
[19] Ulrike Lagerpusch, Volker Mohles, Eckhard Nembach. On the additivity of solid solution and dispersion strengthening [J]. Mater Sci Eng 2001;A319–21:176–8.